Journal of Electrical Bioimpedance
www.bioimpedance.net

J Electr Bioimp, vol. 2, pp. 64–71, 2011
Received: 22 Jul 2011, published: 7 Sep 2011
doi:10.5617/jeb.196

Dielectrophoretic Characterisation of Mammalian Cells above 100 MHz

Colin Chung [1,4], Martin Waterfall [2], Steve Pells [3], Anoop Menachery [1], Stewart Smith [1] and Ronald Pethig [1,4]

1. *Institute for Integrated Micro & Nanosystems, School of Engineering, University of Edinburgh*
2. *Institute of Immunology & Infection Research, School of Biological Sciences, University of Edinburgh*
3. *MRC Centre for Regenerative Medicine, Chancellor's Building, Edinburgh*
4. *E-mail any correspondence to: colin.chung@ed.ac.uk or ron.pethig@ed.ac.uk*

Abstract
Dielectrophoresis (DEP) is a label-free technique for the characterization and manipulation of biological particles - such as cells, bacteria and viruses. Many studies have focused on the DEP cross-over frequency f_{xo1}, where cells in a non-uniform electric field undergo a transition from negative to positive DEP. Determination of f_{xo1} provides a value for the membrane capacitance from the cell diameter, the means to monitor changes in cell morphology and viability, and the information required when devising DEP cell separation protocols. In this paper we describe the first systematic measurements of the second DEP cross-over frequency f_{xo2} that occurs at much higher frequencies. Theory indicates that f_{xo2} is sensitive to the internal dielectric properties of a cell, and our experiments on murine myeloma cells reveal that these properties exhibit temporal changes that are sensitive to both the osmolality and temperature of the cell suspending medium.

Keywords: Biodielectrics, Cytoplasm Conductivity, Dielectrophoresis, Myeloma Cells, Nucleus conductivity.

Introduction

Dielectrophoresis (DEP) is a technique that has been used to characterize and sort cells based on their distinct dielectric properties [1-3]. It refers to a force induced on polarisable particles in non-uniform electric fields. This force is proportional to both the field gradient and the real part of the particle's effective polarisability (per unit volume), described by the Clausius-Mossotti function:

$$\mathbf{p} = \frac{\varepsilon_p^* - \varepsilon_m^*}{\varepsilon_p^* + 2\varepsilon_m^*} \qquad (1)$$

Here, ε_p^* and ε_m^* refer to the complex effective permittivities of the particle and suspending medium, respectively. Of particular interest to those studying the DEP properties of viable mammalian cells is measurement of the so-called DEP cross-over frequency – where the DEP force acting on a cell transitions from a negative to positive polarity. Measurement of this frequency and the cell diameter provides a determination of membrane capacitance and is typically observed in the 100~300 kHz range [2]. The majority of reported DEP studies have been limited to a maximum frequency of ~30 MHz, primarily reflecting the limitation of most commercially available signal generators in delivering the required voltage (up to ~12 V_{pk-pk}) above this frequency. Under appropriate experimental conditions, a second cross-over is expected to occur at frequencies beyond 100 MHz, measurement of which is expected to reveal information regarding the dielectric properties of the cell interior [3]. To our knowledge no systematic investigation of this high-frequency DEP cross-over has been reported in the literature. In this paper we describe the circuitry and electrical load modeling for an interdigitated electrode array used to obtain, for the first time, measurements of this cross-over for mammalian cells as a function of time, suspending medium osmolality and temperature.

Multi-Shell Dielectric Model of a Cell

The effective dielectric properties of a mammalian cell can be modelled by applying the multi-shell method first described by Irimajiri [4]. The nucleoplasm, nuclear membrane, cytoplasm and cytoplasm membrane are represented as concentric spherical shells with distinct radii and dielectric properties (defined by their permittivity and conductivity). By successively merging these shells together an expression for the effective complex permittivity of an entire cell can be produced. Asami *et al* [5] used this method to determine the dielectric properties of mouse lymphocytes, based on impedance measurement of their suspensions. Inserting the dielectric parameters for these lymphocytes into equation 1 gives the DEP frequency response shown in figure 1.

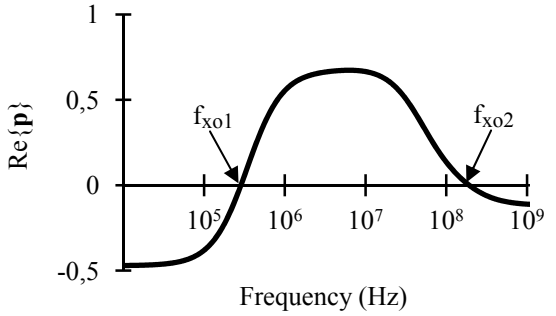

Fig.1: Frequency variation of the real part of the Clausius-Mossotti function for lymphocytes, derived from published dielectric data [5]. The DEP force is proportional to this function and shows two cross-over frequencies, f_{xo1} and f_{xo2}.

We use the form of figure 1 as a predictive guide to the DEP response of mammalian cells. The frequency regions exhibiting negative and positive DEP force correspond respectively to repulsion from, and attraction to, regions of high electric field concentration that occur close to the edge of electrodes. Between 100 kHz and 1 MHz this force transitions from negative to positive at the first (low frequency) cross-over frequency, f_{xo1}. The value of f_{xo1} depends upon the cytoplasm membrane capacitance and resistance, the cell diameter and the suspending medium conductivity [2, 6]. Determination of f_{xo1} for different cells and cell states has been the principle parameter for characterizing and sorting cells by DEP. In figure 1 it can also be seen that, at a frequency between 100 MHz and 1 GHz, a second cross-over, f_{xo2}, is predicted to occur. Above 100 MHz the membrane capacitive reactance should effectively short out the membrane resistance, so that the electric field penetrates into the cell interior [3]. The value of f_{xo2} for viable cells is thus predicted to depend on the intracellular dielectric properties.

A general expression for determining the DEP cross-over frequencies is derived by equating the real part of equation 1 to zero. This yields equation 2, where ε_m and σ_m represent the permittivity and conductivity of the suspending medium; ε_c and σ_c the effective permittivity and conductivity of the cell [7]:

$$f_{xo} = \frac{1}{2\pi}\sqrt{\frac{(\sigma_m - \sigma_c)(\sigma_c + 2\sigma_m)}{(\varepsilon_c - \varepsilon_m)(\varepsilon_c + 2\varepsilon_m)}} \quad (2)$$

The customary practice is to employ the DC approximations derived by Schwan [8] for the low-frequency effective values of σ_m and ε_m – namely $\sigma_m = rG_m$ and $\varepsilon_m = rC_m$, where G_m and C_m are the conductance and capacitance, respectively, of the cell membrane, and r is the cell radius. This leads to a simple expression for f_{xo1}, from which values of the membrane capacitance and conductance can be derived [2, 6]. Above ~1 MHz, and certainly for the high frequencies of relevance to the work reported here, the DC approximations are not applicable. Instead, the frequency dependencies of the effective permittivity and conductivity of a cell must be taken into account. This can be accomplished using the multi-shell model, described in the Appendix, which with simplifying assumptions yields equations 3 and 4 that can be used to determine f_{xo2}:

$$\varepsilon_c \approx \varepsilon_{cp}\frac{2(1-v)+\frac{\varepsilon_{np}}{\varepsilon_{cp}}(1+2v)}{(2+v)+(1-v)\frac{\varepsilon_{np}}{\varepsilon_{cp}}} \quad (3)$$

$$\sigma_c \approx \sigma_{cp}\frac{2(1-v)+\frac{\varepsilon_{np}}{\varepsilon_{cp}}(1+2v)}{(2+v)+(1-v)\frac{\varepsilon_{np}}{\varepsilon_{cp}}} - \left(\frac{\varepsilon_{np}\sigma_{cp}-\varepsilon_{cp}\sigma_{np}}{\varepsilon_{cp}}\cdot\frac{9v}{\left[(2+v)+(1-v)\frac{\varepsilon_{np}}{\varepsilon_{cp}}\right]^2}\right) \quad (4)$$

From equations 3 and 4 we find that the high frequency DEP cross-over f_{xo2} is determined by the internal cell dielectric parameters, namely the nucleoplasm permittivity (ε_{np}), nucleoplasm conductivity (σ_{np}), cytoplasm permittivity (ε_{cp}), cytoplasm conductivity (σ_{cp}) and nucleus volume fraction (v = nucleus volume/cell volume). Based on dielectric studies of mouse lymphocyte suspensions, Asami *et al* [5] derived the following dielectric values: nucleoplasm relative permittivity 52; nucleoplasm conductivity 1.35 S/m; cytoplasm relative permittivity 60; cytoplasm conductivity 0.32 S/m. Substituting these values into equations 2, 3 and 4, for the medium conductivity of 33 mS/m used in our experiments, we can predict a value for f_{xo2} in the range 90 to 320 MHz depending on the nucleus volume fraction.

Materials and methods

Interdigitated electrodes are commonly used in DEP experiments, but understanding their behaviour above 100 MHz requires accurate modelling of the electrical load being driven by the signal source. An overview of the electrical system used to conduct f_{xo2} measurements is shown in figure 2. The signal generator provides a sine wave between 2 MHz and 500 MHz at up to 2 $V_{pk\text{-}pk}$. This is fed to a high power amplifier with ~17.5 dB gain over this range when terminated into a 50Ω load. A 50Ω resistor in parallel with the DEP electrodes is used to approximate this termination, connected by a short ¼ metre length of co-axial cable. This prevents reflection issues with longer cables that reduce bandwidth. The interdigitated structure is fabricated from 100nm thick platinum deposited onto a Pyrex substrate, patterned using standard photolithographic techniques and etched by argon plasma milling.

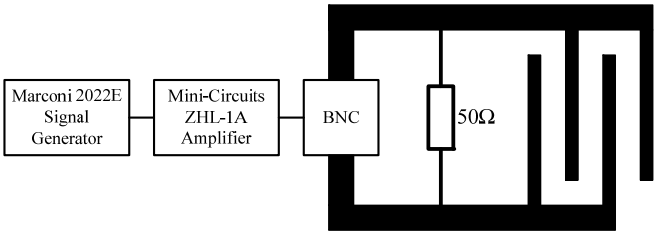

Fig.2: Schematic of the electrical system used to investigate the DEP properties of cells above 100 MHz.

Two interdigitated electrode 'fingers' are shown in figure 3, with a signal being applied to the left pad and grounded on the right pad. An example of a current path is displayed in red, flowing from the signal pad and along the top finger track. At some point this current crosses through the suspending medium to the bottom finger, along the remaining track to ground. A continuum of such current paths exist along the overlap length (L_O), determined by track resistance, suspending medium conductivity and capacitive coupling between the fingers.

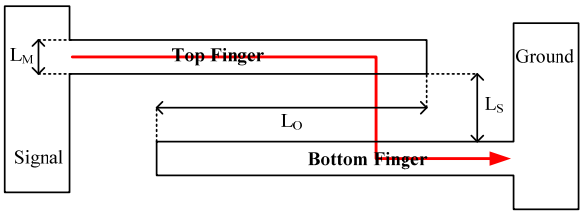

Fig.3: Interdigitated electrode fingers and example current path.

The distributed RCR network of figure 4 has been used to model these parameters. Track resistance (R_t), suspending medium resistance (R_s) and parallel track capacitance (C) components were used for sections of length Δx - L_O divided by the number of sections. Sheet resistance from cross bridge resistor measurements was used to estimate R_t. Values for R_s and C per unit length along the fingers were determined by finite element models of a cross section in COMSOL Multiphysics software. The accuracy of this distributed network increases as Δx approaches zero, but beyond five sections the differences between impedance spectra were observed to be marginal. Ten sections were used to provide sufficient detail for voltage distribution plots.

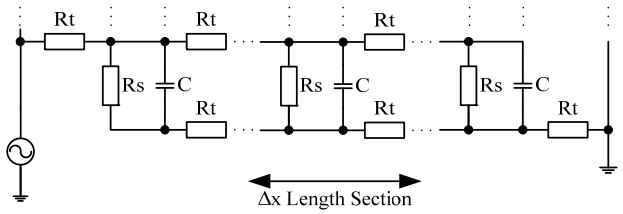

Fig.4: Distributed RCR interdigitated electrode model.

The voltage difference between the adjacent fingers creates the non-uniform electric field *E*, inducing a DEP force upon the cells. The DEP force is proportional to ∇E^2, and needs to be maintained along the entire electrode structure at all frequencies of interest to ensure that cells, which have transitioned from negative to positive DEP, become attracted to the electrode edge in a practical time period, typically less than 10 seconds. At the 20µm electrode scale, for the purpose of DEP cross-over measurement, a minimum voltage difference of 3.5 $V_{pk\text{-}pk}$ was found to be sufficient. The signal generator was adjusted for the amplifier to output 5 $V_{pk\text{-}pk}$ when terminated into 50Ω.

Specifications for two examples of interdigitated electrodes are given in table 1, fabricated from 50 and 100 nm thick platinum.

	Design 1	Design 2	
Number of Fingers	16	16	
Finger Overlap (L_O)	20	2	mm
Finger Width (L_W)	20	25	µm
Finger Spacing (L_S)	20	35	µm
Medium Conductivity	33	33	mS/m
Sheet Resistance	3.6	1.8	Ω/□
Section Length (Δx)	2	0.2	mm
Section Medium Resistance (R_s)	30	340	kΩ
Section Track Resistance (R_t)	28.8	14.4	Ω
Section Track Capacitance (C)	1500	67	fF
Area	12.8	1.9	mm^2

Tab.1: Model parameters for two electrode design examples.

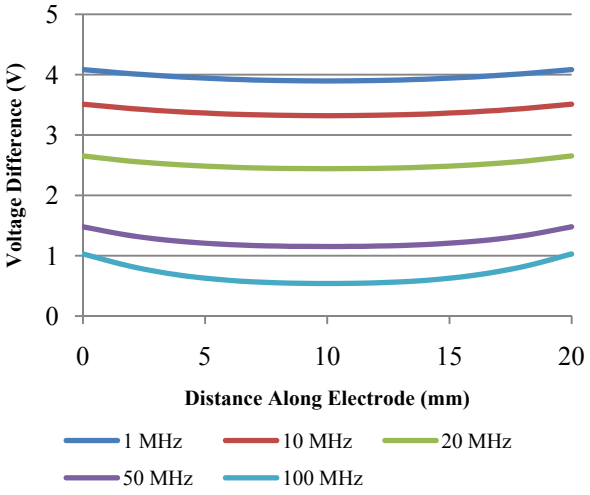

Fig.5: Voltage difference between adjacent fingers (Design 1).

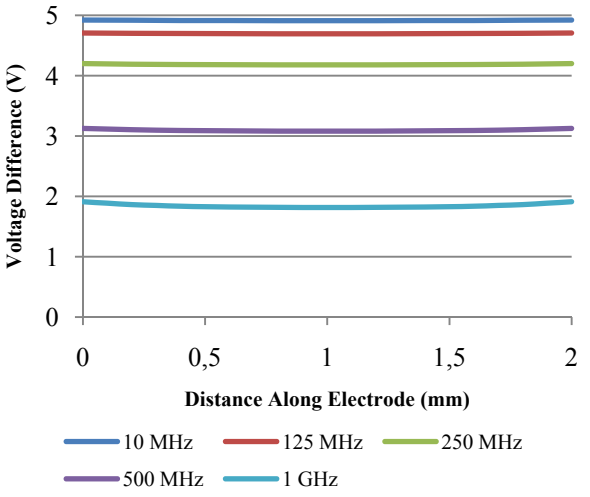

Fig.6: Voltage difference between adjacent fingers (Design 2).

The voltage difference profiles shown in figure 5 take the form of catenaries due to the resistive and capacitive loading along the length of the electrode fingers. The bandwidth, defined by a minimum voltage difference of 3.5V, is only 8 MHz and far below the upper range of 320 MHz predicted for f_{xo2}. Electrode design 2 shown in table 1 features an increased finger width and spacing, which

reduces the finger overlap, and double the platinum thickness. As shown in figure 6, this flattens the voltage difference profile and increases the DEP operating bandwidth to 400 MHz. However, this is achieved at the cost of significantly reducing the electrode area. Electrode design 2 was used for the DEP studies described here.

Cell Culture

Murine myeloma SP2/O cells were grown in RPMI-1640 medium supplemented with 100 units/mL penicillin-streptomycin and 10% foetal calf serum (FCS). The cells were grown in suspension with 5% CO^2 in air at 37°C to a density of $1x10^6$ cells/mL. An iso-osmotic cell suspension medium for DEP studies was prepared by adding 3 g/L glucose and 100 g/L sucrose to DI water. Conductivity was adjusted to 33 mS/m with PBS, verified using a conductivity meter (Oakton CON 510) and the pH adjusted to 7.4 with NaOH/HCl. The osmolality of the final medium was 310 mOsm/kg, verified with an osmometer (Advanced Instruments Inc. Model 3300). DEP media of osmolality 250, 390, 435 and 480 mOsm/kg were also prepared by adjusting the sucrose concentration. The SP2/O cells were centrifuged (100g, 5 minutes) and washed twice in 10 mL of the DEP media, before final suspension at a density of $1x10^7$ cells/mL for analysis. The electrodes were mounted in an inverted microscope (Meiji TC5100). By focusing on the electrode plane discrimination between cells undergoing negative DEP (out-of-focus or between the electrodes) and positive DEP (in-focus at electrode edges) was possible.

Results

Figure 7 shows the distribution of values for the high-frequency crossover, f_{xo2}, with a population sample of 418 SP2/O cells suspended in a DEP medium of osmolality 310 mOsm/kg. Under these conditions the vast majority of cells were observed to undergo the transition from negative to positive DEP when sweeping down the frequency range.

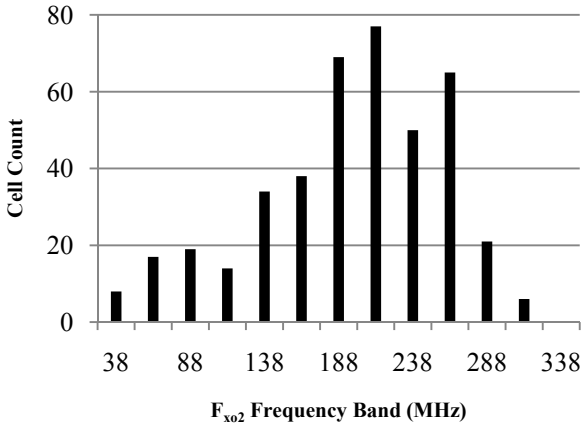

Fig.7: F_{xo2} spectrum for SP2/O cells (n=418) suspended in DEP medium with 310 mOsm/L osmolality and 33 mS/m conductivity.

The mean value of f_{xo2} for the cell populations shown in figure 7 is 195 MHz with a standard deviation of 63 MHz. An interesting finding, shown in figure 8, is the reduction of the f_{xo2} values as a function of time after their suspension in the DEP solution.

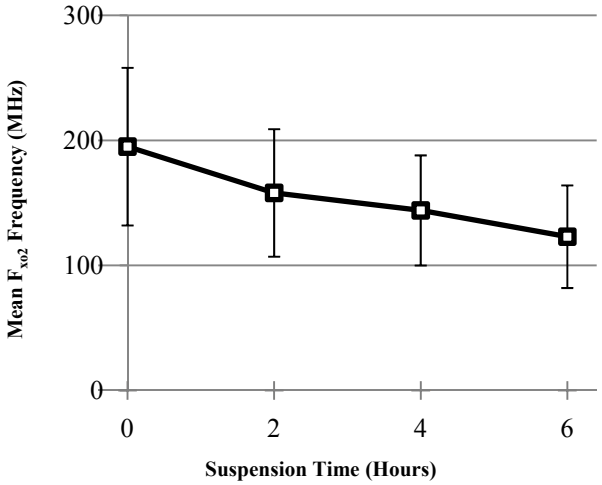

Fig.8: Mean f_{xo2} frequency for SP2/O cells suspended in DEP medium with 310 mOsm/L osmolality and 33 mS/m conductivity over 6 hours. Single standard deviation bars shown.

A corresponding temporal change in the low-frequency cross-over, f_{xo1}, was not observed, and is not expected unless the cell state is deliberately altered by adding chemical agents to the solution known to induce cell activation or apoptosis for example [2, 9].

The reduction in f_{xo2} over time was found to be a function of temperature, as shown in figure 9. Cell suspensions were held in a temperature controlled water bath (situated in a refrigerated room for the 10°C run) between measurements. The rate of frequency reduction based on the first two hours clearly increases with temperature, more than doubling in rate (~2.4x) for increases of 10°C between 21°C and 37°C.

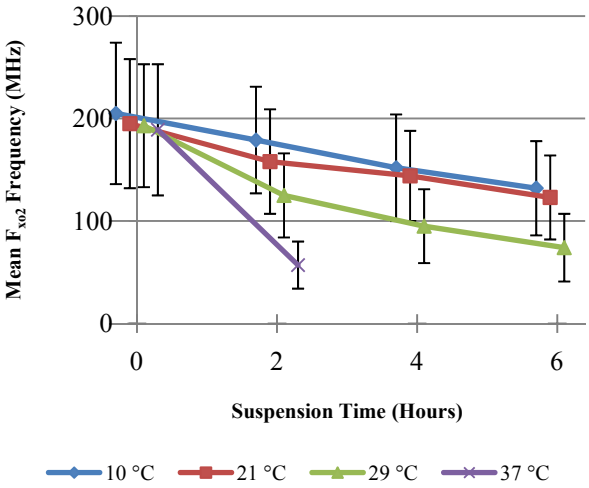

Fig.9: Mean f_{xo2} frequency for SP2/O cells suspended in 310 mOsm DEP medium at 10°C, 21°C, 29°C and 37°C over 6 hours. Single standard deviation bars are shown.

At 37°C the rate of fall of f_{xo2} was so great that accurate determination of it became difficult after two hours. The osmolality of the suspending solution was also found to influence the mean f_{xo2} value, as shown in figure 10. The higher osmolality solutions tended to result in lower values of f_{xo2} for the same period of cell suspension in the DEP solution.

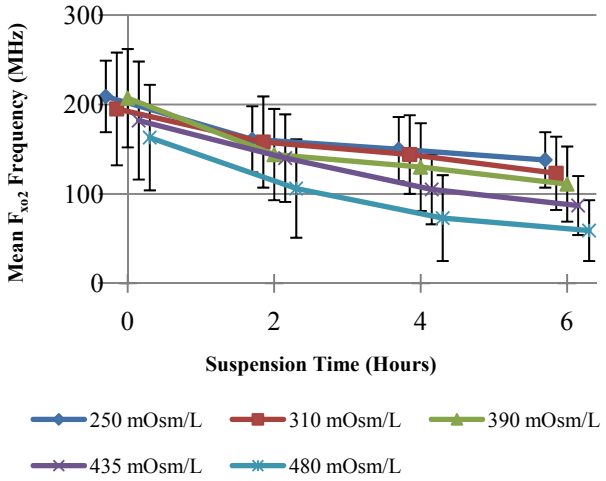

Fig.10: Mean f_{xo2} frequency for SP2/O cells suspended in DEP media of 250, 310, 390, 425 and 480 mOsm/L. Standard deviation bars are shown.

Discussion

The distribution of high frequency cross-over, f_{xo2}, values for SP2/O cells shown in figure 7 was obtained by slowly sweeping down from an applied signal frequency of 400 MHz. At this initial frequency all of the cells were observed to levitate above the electrode plane under the action of negative DEP, but on proceeding below 325 MHz subpopulations of the cells were attracted to the electrode edges by positive DEP. This behaviour confirmed that the predicted high-frequency DEP cross-over shown in figure 1 for mammalian cells can be observed under our experimental conditions, and that the designed electronics and electrodes are capable of exploring this high frequency region of the DEP spectrum. The mean f_{xo2} value of 195 MHz shown in figure 7 falls well within the 90 MHz to 320 MHz range of values we predicted using the cell dielectric parameters given by Asami *et al* [5]. This provides a degree of validation for both the multi-shell model of a cell and our use of the extracted dielectric parameters. Our theoretical analysis - yielding equations 3 and 4 for the effective cell permittivity and conductivity at high frequencies - indicates that f_{xo2} is sensitive to the effective dielectric properties of the cell interior. This distinguishes f_{xo2} from the lower frequency DEP cross-over at f_{xo1} which is sensitive to the suspending medium conductivity, the cell radius, and the effective permittivity and conductivity of the plasma membrane [2, 6, 9]. Extending DEP measurements to include analyses of both f_{xo1} and f_{xo2} should therefore provide enhanced characterisation of the dielectric properties of cells, and enable more efficient manipulations of cells (e.g., subpopulation enrichment or selective separation) using DEP techniques.

Equations 3 and 4 inform us that the high frequency cross-over, f_{xo2}, is determined by the permittivity and conductivity of both the nucleoplasm and cytoplasm, as well as the nucleus volume fraction. The nucleus volume fraction is known to change with cell cycle [10], and could be one factor responsible for the relatively wide distribution of f_{xo2} values shown in figure 7. The relationships of the dielectric parameters to specific biological features of a cell are at present not clear, but an insight into the relative sensitivity of f_{xo2} to them can be obtained.

	Permittivity	**Conductivity**
Medium	31%	0%
Nucleus	8%	13%
Cytoplasm	6%	1%
Nucl. Vol. Fraction	8%	

Tab.2: Sensitivity of f_{xo2} to dielectric parameters based on Asami *et al* [5] for a nucleus volume fraction of 0.7. The change in frequency for a ±10% variation in each parameter is normalised to the base f_{xo2} value of 195 MHz.

Table 2 provides a measure of sensitivity in f_{xo2} to each dielectric parameter based on the modelled values undergoing a +/- 10% variation. A nucleus volume fraction of 0.7 is used here with values approaching ~0.9 being typical of lymphocytes which are associated with our SP2/O cells [11]. Finally, the intracellular conductivity is scaled for a base f_{xo2} value of 195 MHz to which these variations are normalised.

F_{xo2} is unaffected by small changes in medium conductivity although a large increase, beyond ~300 mS/m, results in a collapsed DEP profile with no cross-over occurring. F_{xo2} is most sensitive to the medium permittivity, a parameter which is dependent upon temperature but regulated precisely in these experiments [12]. The conductivity, permittivity and volume fraction of the nucleus are the most likely causes for the temporal change displayed in figure 8. A reduction in f_{xo2} of the magnitude observed requires the effective conductivity of the cell interior to reduce by a factor of nearly 40%. This represents a significant alteration in cell state, and could be directly related to the fact that for our DEP experiments the cells were suspended in low ionic strength solutions, commonly used for the determination of f_{xo1}, for example [2, 6, 9].

Processes that could be responsible for the temporal reduction in f_{xo2} reported here could include the leakage of

ions, such as potassium, down their concentration gradients to the cell exterior, or the osmotic flux of water across the plasma membrane [13]. Such changes would not influence measurements of the lower frequency DEP cross-over at f_{xo1}, unless they lead to significant changes in cell volume, morphology or viability [2, 3, 9]. Determination of the temporal behaviour of f_{xo2} may prove to be a sensitive indicator of loss of cell viability, and a useful tool to be used when formulating the chemical composition of cell suspending media to be used in DEP studies [14].

Q_{10} is a widely used quantity in the study of metabolic activity and is the factor by which a 10°C increase in temperature alters a reaction rate [15, 16]. The temperature dependence results shown in figure 9 suggest Q_{10} is approximately 2.4 for the process in question, between 21°C and 37°C; and within the typical range for biological processes. Based on this data, the Arrhenius plot of figure 11 provides further detail regarding this process.

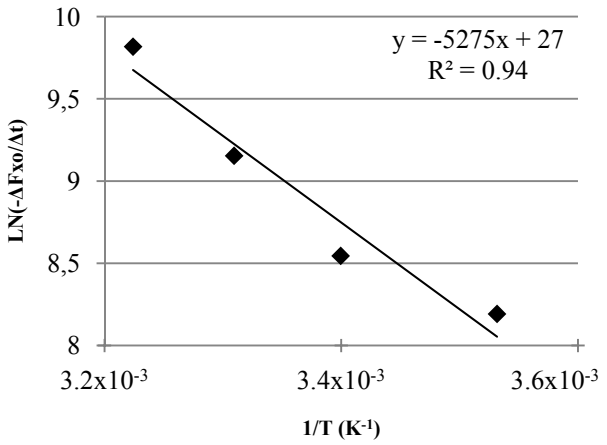

Fig.11: Arrhenius plot for the initial rate of mean f_{xo2} roll-off.

The linear fit of the data gives an activation energy of ~44 kJ/mol for the underlying process leading to the temporal behaviour of the high frequency DEP cross-over. We note that the temperature dependence of the coefficient of water self-diffusion through lipid multilayers is also described by the Arrhenius law, with an apparent activation energy of ~41 kJ/mol [17], a coincidence which requires further study.

Finally, the trend shown in figure 10, of a decrease in f_{xo2} with increasing osmolality of the cell suspending medium, suggests an associated decrease in internal cell conductivity and/or permittivity. The mechanism for this may be related to that of the aforementioned temporal reduction in frequency, however the initial rate of reduction appears to be unaffected by the change in osmotic pressure.

Conclusions

An electrical system comprising interdigitated electrodes and signal generator has been designed and tested to observe, for the first time, cells undergoing DEP cross-over in the predicted frequency range above 100 MHz. Electrical modelling of the electrodes based on a distributed RCR network allowed us to determine the limiting factors for high frequency operation. Capacitive loading is the most critical factor, and results in an imposed limitation of the electrode area. The mean f_{x02} value of 195 MHz observed for murine myeloma SP2/0 cells agrees well with that predicted using the cell interior dielectric properties derived from impedance studies of lymphocytes [5]. This suggests that the internal dielectric properties derived from lymphocytes, and the multi-shell model of a cell, may be applicable for the study of other mammalian cell types using the electrodes and electronics described here.

The theory indicates that the high frequency DEP cross-over at f_{x02} is sensitive to changes in the dielectric properties of the cell interior, and especially those associated with the nucleus and the relative size of the nucleus to the cell volume. An interesting finding, and one not predicted from the large number of reported studies of the low frequency DEP cross-over at f_{x01}, is the rapid reduction of f_{x02} with time. At present we do not understand the changes of cell state that are responsible for this behaviour. Experiments to gain a further understanding are currently in progress in our laboratories. One important conclusion to be drawn is that measurements of both the low and high frequency DEP cross-over, at f_{x01} and f_{x02}, are likely to provide a better indicator of any changes in cell state during DEP experiments than through determination of f_{x01} alone. This could be of particular importance for DEP studies and manipulations of stem cells [18].

Acknowledgements

The authors thank Dr Martin Reekie for helpful discussions. This work was supported by a Wolfson Microelectronics Scholarship awarded to C.C., and the Edinburgh Research Partnership in Engineering and Mathematics (ERPem).

References

1. Voldman J. Electrical Forces for Microscale Cell Manipulation. Annu. Rev. Biomed. Eng. 2006:8:p. 425-54. doi: 10.1146/annurev.bioeng.8.061505.095739
2. Pethig R, Talary MS. Dielectrophoretic Detection of Membrane Morphology Changes in Jurkat T-Cells Undergoing Etoposide-Induced Apoptosis. IET Nanobiotechnol. 2007:1:p. 2-9. doi: 10.1049/iet-nbt:20060018
3. Pethig R. Review Article – Dielectrophoresis: Status of the Theory, Technology and Applications. Biomicrofluidics 2010:4:022811. doi: 10.1063/1.3456626
4. Irimajiri A. A Dielectric Theory of "Multi-Stratified Shell" Model with its Application to a Lymphoma Cell. J. Theor. Biol. 1979:78:p. 251-69. doi: 10.1016/0022-5193(79)90268-6

5. Asami K, Takahashi, Y, Takashima S. Dielectric Properties of Mouse Lymphocytes and Erythrocytes. Biochim. Biophys. Acta 1989:1010:p. 49-55. doi: 10.1016/0167-4889(89)90183-3
6. Pethig R, Jakubek LM, Sanger RH, Heart E, Corson ED, Smith PJS. Electrokinetic Measurements of Membrane Capacitance and Conductance for Pancreatic Beta-cells. IEE Proc. Nanobiotechnol. 2005:152:6:p. 189-193. doi: 10.1049/ip-nbt:20050040
7. Jones T. Electromechanics of Particles. Cambridge University Press; 1995. p. 56. doi: 10.1017/CBO9780511574498
8. Schwan, H.P., Electrical properties of cells and tissues, Adv. Biol. Med. Phys., 1957, 5, pp. 147-209.
9. Wang X, Becker FF, Gascoyne PRC. Membrane Dielectric Changes Indicate Induced Apoptosis in HL-60 Cells More Sensitively Than Surface Phospatidylserine Expression or DNA Fragmentation. Biochim. Biophys. Acta 2002:1564:p. 412-420. doi: 10.1016/S0005-2736(02)00495-9
10. 10. Turgeon ML. Clinical Hematology: Theory and Procedures. Lippincott, Williams & Wilkins:2005. p. 67.
11. CAP Proficiency Testing Handbook:1995. Secton 2, Hematology, Coagulation, Clinical Microscopy.
12. Catenaccio A, Daruich Y, Magallanes C. Temperature Dependence of the Permittivity of Water. Chem. Phys. Lttrs 2003:367:p. 669-671. doi: 10.1016/S0009-2614(02)01735-9
13. Ho SN. Intracellular Water Homeostasis and the Mammalian Cellular Osmotic Stress Response. J. Cell. Phys 2006:206:p. 9-15. doi: 10.1002/jcp.20445
14. Puttaswamy SV, Sivashankar S, Chen RJ, Chin CK, Chang HY, Cheng HL. Enhanced Cell Viability and Cell Adhesion Using Low Conductivity Medium for Negative Dielectrophoretic Cell Patterning. Biotechnol. J. 2010:5:p. 1005-1015. doi: 10.1002/biot.201000194
15. Lehninger AL. Biochemistry. 2nd ed. Worth Publishers, Inc; 1975. p. 196.
16. Bekku YS, Nakatsubo T, Kume A, Adachi M, Koizumi H. Effect of Warming on the Temperature Dependence of Soil Respiration Rate in Arctic, Temperate and Tropical Soils. Appl. Soil Ecol. 2003:22:p. 205-210. doi: 10.1016/S0929-1393(02)00158-0
17. Khakimova AM, Rudakova MA, Doroginitskiĭ MM, Filippov AV. An NMR Study of the Temperature Dependence of the Coefficient of Water Self-Diffusion through Lipid Bilayer Membranes. Biofizika. 2008:53(2):p. 271-80.
18. Pethig R, Menachery A, Pells S, De Sousa P. Dielectro-phoresis: A Review of Applications for Stem Cell Research, J. Biomed. Biotechnol., 2010:182581 (7 pages). doi: 10.1155/2010/182581

Appendix

Calculating the DEP cross-over frequency using equation 2 requires both the effective permittivity and effective conductivity of the particle. These need to account for both geometric and dielectric properties which, for suspended mammalian cells, may be modelled by a multi-shelled sphere [4, 5]. Defining first these properties for each shell consisting of the following elements:

	Radius (r) / Thickness (t)	Complex Permittivity
Nucleoplasm	r_{np}	ε^*_{np}
Nuclear Envelope	t_{ne}	ε^*_{ne}
Cytoplasm	r_{cp}	ε^*_{cp}
Cell Membrane	t_{mb}	ε^*_{mb}

Each complex permittivity is composed of permittivity, ε, and conductivity, σ, with angular frequency, ω, and imaginary unit, i, by the relationship:

$$\varepsilon^*_{xx} = \varepsilon_{xx} - \frac{i}{\omega}\sigma_{xx}$$

We define the cell's effective permittivity, ε^*_c, in terms of the following intermediate parameters, E_x, and volume fractions, v_x:

$$\varepsilon^*_c = \varepsilon^*_{mb}\frac{2(1-v_1)+(1+2v_1)E_1}{(2+v_1)+(1-v_1)E_1} \qquad v_1 = \left(1-\frac{t_{mb}}{r_{cp}}\right)^3$$

$$E_1 = \frac{\varepsilon^*_{cp}}{\varepsilon^*_{mb}}\frac{2(1-v_2)+(1+2v_2)E_2}{(2+v_2)+(1-v_2)E_2} \qquad v_2 = \left(\frac{r_{np}}{r_{cp}-t_{mb}}\right)^3$$

$$E_2 = \frac{\varepsilon^*_{ne}}{\varepsilon^*_{cp}}\frac{2(1-v_3)+(1+2v_3)E_3}{(2+v_3)+(1-v_3)E_3} \qquad v_3 = \left(1-\frac{t_{ne}}{r_{np}}\right)^3$$

$$E_3 = \frac{\varepsilon^*_{np}}{\varepsilon^*_{ne}}$$

Real solutions for equation 2 for a suspending medium of permittivity, ε_m, and conductivity, σ_m, must satisfy the condition [7]:

$$\frac{\sigma_m - \sigma_c}{\varepsilon_c - \varepsilon_m} > 0$$

Asami *et al* [5] derived the following dielectric parameters for mouse lymphocytes: r_{np} = 2.6 μm; t_{ne} = 40 nm; r_{cp} = 2.9 μm; t_{mb} = 7 nm; $\varepsilon_{np} = 52\varepsilon_0$; $\varepsilon_{ne} = 28\varepsilon_0$; $\varepsilon_{cp} = 60\varepsilon_0$; $\varepsilon_{mb} = 6.8\varepsilon_0$; σ_{np} = 1.35 S/m; σ_{ne} = 6 mS/m; σ_{cp} = 0.32 S/m; σ_{mb} = 3.2 μS/m. Substituting these values into the expressions above, with σ_m = 33 mS/m and $\varepsilon_m = 80.1\varepsilon_0$, yields the effective conductivity and relative permittivity spectra of figure A1. The form of these spectra imply that real solutions for equation 2 exist below 5 MHz and above 120 MHz. Applying the simplification that $t_{ne} \approx 0$, and eliminating terms divided by ω^2 we obtain a simplified, high-frequency, expression for E_2:

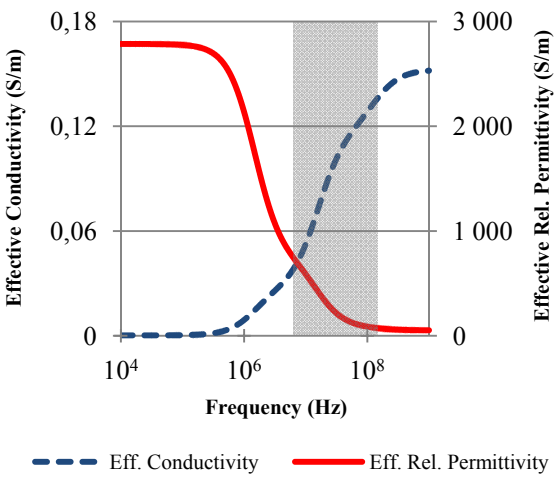

Fig.A1: Effective conductivity and relative permittivity of a cell based on the dielectric data of Asami *et al* [5]. The dark band indicates where real solutions for the DEP cross-over do not exist.

$$E_2 = \frac{\varepsilon_{cp}\varepsilon_{np} + \frac{\sigma_{cp}\sigma_{np}}{\omega^2}}{\varepsilon_{cp}^2 + \frac{\sigma_{cp}^2}{\omega^2}} + i\frac{\frac{\varepsilon_{np}\sigma_{cp}}{\omega} - \frac{\varepsilon_{cp}\sigma_{np}}{\omega}}{\varepsilon_{cp}^2 + \frac{\sigma_{cp}^2}{\omega^2}}$$

$$\approx \frac{\varepsilon_{np}}{\varepsilon_{cp}} + i\frac{\varepsilon_{np}\sigma_{cp} - \varepsilon_{cp}\sigma_{np}}{\omega\varepsilon_{cp}^2} \stackrel{\text{def}}{=} X_1 + iX_2$$

For the sake of clarity we define the real and imaginary parts, respectively, as X_1 and X_2 here. Substituting these into E_1 with $t_{mb} = 0$ yields an expression for ε_c^* where terms involving $X_2^2 \propto \omega^{-2}$ can be eliminated.

$$\varepsilon_c^* \approx \varepsilon_{cp}^* \left[\frac{2(1-v_2) + X_1(1+2v_2)}{(2+v_2) + (1-v_2)X_1}\right.$$

$$+i\frac{X_2(1+2v_2)[(2+v_2) + (1-v_2)X_1]}{[(2+v_2) + (1-v_2)X_1]^2}$$

$$\left.-i\frac{X_2(1-v_2)[2(1-v_2) + X_1(1+2v_2)]}{[(2+v_2) + (1-v_2)X_1]^2}\right]$$

Expanding out ε_{cp}^*, substituting back for X_1 and X_2 and rearranging ε_c^* into the general form of complex permittivity gives:

$$\varepsilon_c^* \approx \varepsilon_{cp}\frac{2(1-v_2) + \frac{\varepsilon_{np}}{\varepsilon_{cp}}(1+2v_2)}{(2+v_2) + (1-v_2)\frac{\varepsilon_{np}}{\varepsilon_{cp}}}$$

$$-i\left[\frac{\sigma_{cp}}{\omega}\cdot\frac{2(1-v_2) + \frac{\varepsilon_{np}}{\varepsilon_{cp}}(1+2v_2)}{(2+v_2) + (1-v_2)\frac{\varepsilon_{np}}{\varepsilon_{cp}}}\right.$$

$$\left.-\varepsilon_{cp}\frac{\varepsilon_{np}\sigma_{cp} - \varepsilon_{cp}\sigma_{np}}{\omega\varepsilon_{cp}^2}\cdot\frac{9v_2}{\left[(2+v_2) + (1-v_2)\frac{\varepsilon_{np}}{\varepsilon_{cp}}\right]^2}\right]$$

Comparing the coefficients with the general form for complex permittivity, the real part of this expression corresponds to the effective cell permittivity of equation 3. The imaginary part, multiplied by -ω/i, corresponds to the effective cell conductivity of equation 4.